

Effects of W on high-temperature antioxidative properties of Nb/Nb₅Si₃ composite

Long Wenyuan^a, Liu Weiguo^b, Liu Xuan^c

College of Aeronautical Manufacturing Engineering, Nanchang Hangkong University, Nanchang 330063, China

^aemail: long_weny@163.com, ^bemail: 514863450@qq.com, ^cemail: 1300908643@qq.com

Keywords: Spark plasma sintering; In-situ synthesis; Oxidation behaviour; Nb/Nb₅Si₃ composites

Abstract. The multi-component Nb-Si system in-situ composites with composition of Nb-20Si-5Al-15Ti-xW (at. %) were prepared by Spark Plasma Sintering (SPS) technology. The high temperature oxidation behavior and microstructure of the alloy were investigated by scanning electron microscopy (SEM), X-ray diffraction (XRD) and electron probe microscopy (EPMA). The results show that the microstructure of the composite consists of (Nb, Ti, W)_{ss}, α-Nb₅Si₃, γ-Nb₅Si₃ and (Nb, Ti, W)₅Si₃ phase. With an increase of W addition, the oxidation resistance of the composites at 800°C decrease firstly and then increase. At 1100°C the addition of W decreased the oxidation resistance during the first 40h, then changed to increase the oxidation resistance. Pest oxidation behavior was exhibited by the Nb-20Si-5Al-15Ti-xW. The oxidation resistance of the composite at 1100°C is better than at 800°C because the oxide scale is more compact structure.

Introduction

Nb-Si alloys are considered attractive for possible replacement of Ni-base super alloys for high temperature (>1100°C) applications[1]. Excellent mechanical properties have been achieved during the development of Nb_{SS}/Nb₅Si₃ composites [2-5]; The best compositions have fracture toughness values exceeding 20MPa·m^{1/2}[2,5]. However, their poor oxidation resistance at intermediate and high temperatures is a major obstacle to their use in high temperature applications.

Now many efforts have been devoted to looking for alloying elements and optimizing their content to enhance the onxidation behavior. Previous work has shown that the oxidation resistance of the Nb/Nb₅Si₃ in situ composites can be improved significantly by additions such as Cr, Al, Ti, Mo and Hf [1,6–10]. Germanium and B additions, as a partial replacement of Si, also improve the oxidation behaviour of Nb/Nb₅Si₃ in-situ composites [3]. However, refractory metals and their alloys can suffer from pest damage at intermediate temperatures (< 850°C) [11-13]. Recent works [3, 14-18] reported beneficial effects of adding tin to Nb/Nb₅Si₃ composites, which delayed the pest phenomena at 800°C. This effect was also beneficial at 1200°C[14,15]. In contrast, Bewlay et al. [3] reported that tin had a minor effect on oxidation resistance at high temperatures. Unfortunately, the level of alloying required for the improvement of oxidation resistance could sacrifice the room temperature fracture toughness and high temperature strength of the composites. Therefore, further investigations are needed to achieve the required balance of oxidation performance and mechanical properties.

In this study, the Nb/Nb₅Si₃ in situ composites were fabricated by SPS technology. This study aims to determine the effect of W on the antioxidative performance of Nb/Nb₅Si₃ composite materials in static air at 800°C and 1100°C.

Experimental conditions and methods

Powders of Nb(99.9wt.%, -200 mesh), Si(99.9wt.%, -300 mesh), Al(99.8wt.%, -100 mesh), Ti(99.8wt.%, -200 mesh), and W(99.9wt.%, -300 mesh) were used as raw materials. The Nb-20Si-5Al-15Ti(at.%), Nb-20Si-5Al-15Ti-5W(at.%) and Nb-20Si-5Al-15Ti-8W(at.%) composites were prepared by SPS in a vacuum atmosphere. The powders were dry-mixed in a

mechanical mixer for 24h, and the mixed powders were packed into a graphite die with an inside diameter of 20mm. The sintering was carried out on a SPS machine manufactured by Sumitomo Coal Mining Co. Ltd., Japan. A uniaxial load of 11kN was applied on the powders to realize sintering and densification simultaneously. A heating speed of 150°C/min and the sintering temperature of 1500°C were adopted under fixed sintering holding time of 10 min.

Samples (6mm×6mm×6mm) for the oxidation experiment were cut by an electro-discharge cutting machine (EDM). The rectangular shape specimens were polished to 1500 grit SiC paper and cleaned in ethanol and acetone. Isothermal oxidation experiments of the rectangular samples were undertaken at 800°C and 1100°C. After each oxidation experiment, the recorded data for weight changes were plotted as weight change per unit surface area as a function of time to determine the oxidation kinetics.

The microstructures were examined using a MeF-3 optical microscope and a JSMT-200 scanning electron microscope (SEM). X-ray diffraction (D/MAX-IIIB) patterns of the bulk specimens were obtained to identify the phases. The distribution of phase and chemical species has been analyzed using JXA-800R electron microprobe analysis.

Results and Discussion

Fig.1 shows the SEM image of Nb/Nb₅Si₃ composite prepared via SPS. The EDS results are shown in Table 1. The bright particle phase in Fig.1(a) (point A) contains Nb, Al, and Ti, and the black particle phase in Fig.1(a) (point C) contains Nb, and Ti, whereas the dark matrix (point B) contains both Nb, Si Al, and Ti(Table 1). The EDS results (Table 1) indicate that the ratio of Nb atoms to Si atoms in the dark matrix (point B) is approximately 5:3. Fig.1(b) and (c) show that point A contains Nb, point B and point C contain Nb, Si, Ti, and W.

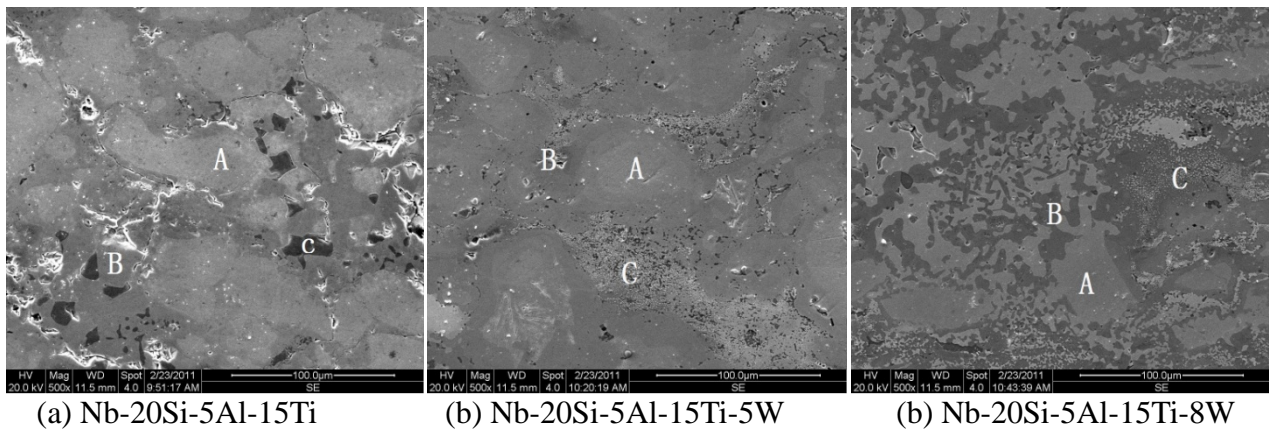


Fig.1 SEM images of Nb/Nb₅Si₃ composites.

Table 1 The results of analysis in EDS

EDS point	Chemical composition (at.%)					
	Nb	Si	Al	Ti	W	
Nb-20Si-5Al -15Ti	A	79.49	0.00	3.20	17.31	
	B	55.62	30.32	1.56	12.49	
	C	6.10	0.00	0.00	93.90	
Nb-20Si-5Al -15Ti-5W	A	74.17	2.24	15.77	6.01	1.81
	B	55.77	19.69	9.45	12.76	2.32
	C	24.52	24.52	3.38	29.25	18.26
Nb-20Si-5Al -15Ti-8W	A	62.65	0.00	6.64	26.29	4.42
	B	32.46	26.64	3.65	37.24	0.00
	C	28.34	17.55	5.33	37.04	11.74

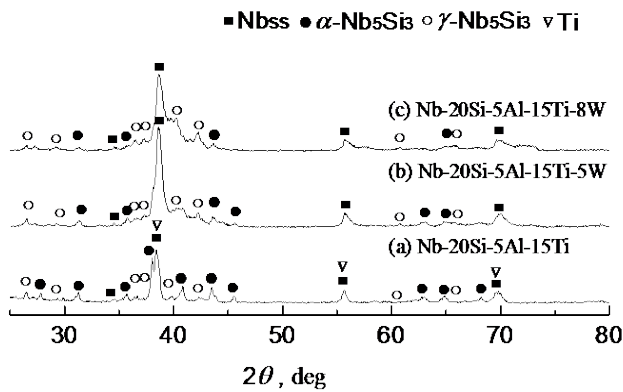


Fig.2. XRD patterns of the sample

The XRD patterns of Nb-20Si-5Al-15Ti, Nb-20Si-5Al-15Ti-5W and Nb-20Si-5Al-15Ti-8W are shown in Fig.2. According to the XRD and EPMA results, the Nb-20Si-5Al-15Ti comprised of Nb_{SS}, Nb₅Si₃ and Ti phases; however, the Nb-20Si-5Al-15Ti-xW comprised of Nb_{SS}, Nb₅Si₃, Ti, W, and Al solubilized in Nb_{SS} and Nb₅Si₃. It is evident that the effects of W on the microstructure of Nb/Nb₅Si₃ in situ composites are inconspicuous and the microstructure is not changed.

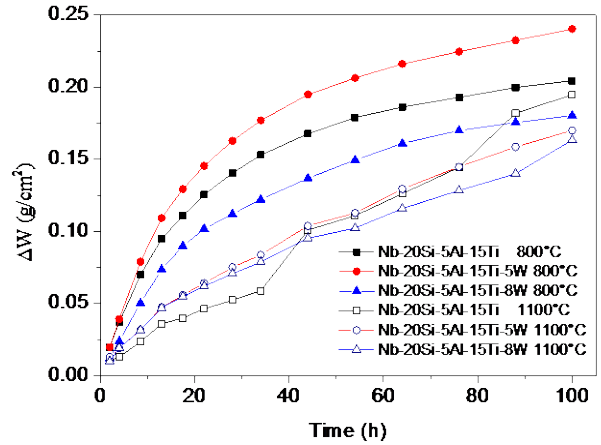


Fig.3. Weight gain curve of sample

The oxidation rates of the composites were measured at 800°C and 1100°C in static air. The thermo-gravimetric results are shown in Fig.3, in which the weight change (g/cm^2) was plotted as a function of oxidation time (s). The weight changes of Nb-20Si-5Al-15Ti-3Cr-xW at 800°C followed parabolic oxidation kinetics, while the oxidation kinetics of Nb-20Si-5Al-15Ti-3Cr-xW at 1100°C are linear, and the oxidation rate are much smaller than that at 800°C. The pest oxidation behaviour is eliminated. With an increase of W addition, the oxidation resistance of the composites at 800°C decreases firstly and then increases. Therefore the Nb-20Si-5Al-15Ti-3Cr-5W composite which exhibited the highest weight gain, showed very poor oxidation behaviour at 800°C. In the presence of 8 at% W, the composite showed better oxidation resistance. At 1100°C the addition of W decreased the oxidation resistance during the first 40h, and then changed to increase the oxidation resistance.

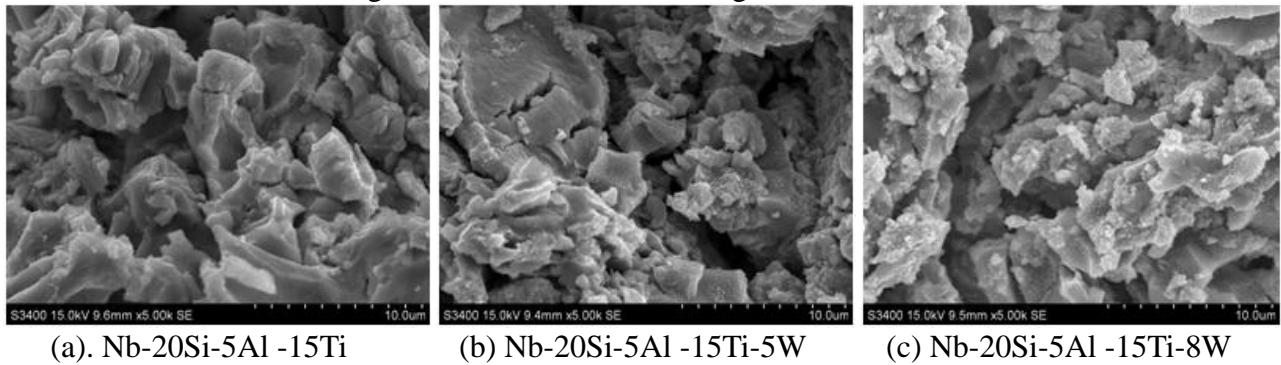


Fig.4 SEM photographs of the oxidized products at 800°C/100 h.

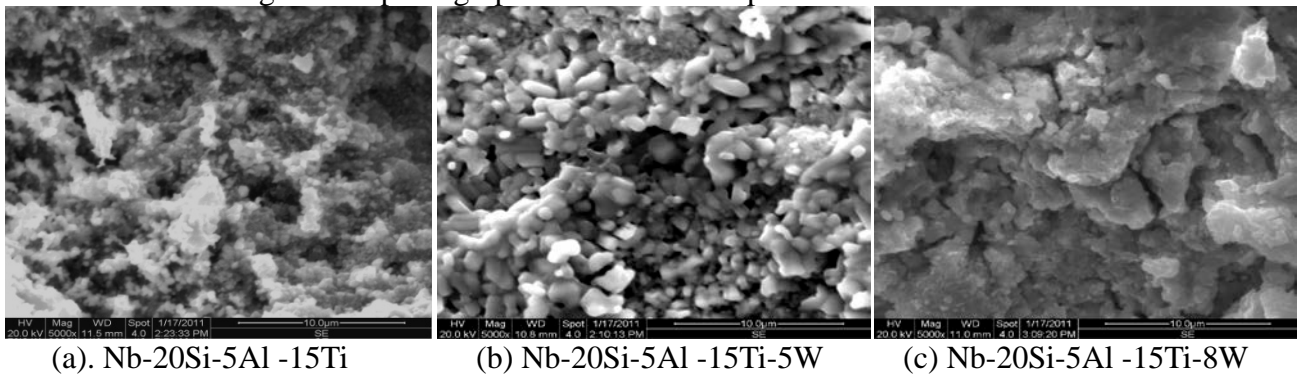


Fig.5 SEM photographs of the oxidized products at 1100°C/100 h.

Based on the Nb-20Si-5Al-15Ti-3Cr-xW composites oxidation weight experiment at 800 and 1100 °C, the composites were completely oxidized after exposure in air for ~60 h at 800 °C, and the

quality of the composites didn't change significantly at the late stage of the test. The composites were not completely oxidized after being exposed to air for 100 h at 1100 °C. The high-temperature antioxidation of the Nb/Nb₅Si₃ composites without alloying are very poor. The high-temperature oxidation resistance is improved by multi-element alloying, particularly at 1100°C, which is better than that at 800°C.

SEM image of the composites oxidized products are presented in Fig.4 and Fig. 5. Fig.4 shows that the oxidized products are amplified by 5,000 times after being oxidized at 800°C/100h. The oxidized products are mainly lamellar. The oxidized products are porous and contained numerous microcracks. Fig.5 shows that the oxidized products are amplified 5,000 times after oxidation at 1100°C/100h. The particle size of the oxidized products are uniform and have a compact arrangement with some holes, which affects the antioxidant property: the antioxidant properties of the composites at 1100°C were significantly superior to that at 800 C. This result is due to that the oxidized products of composite at 1100°C are more compact, thereby reducing the direct contact of oxygen with the base material. In addition, a relatively uniform particle size distribution is achieved compared a smooth sheet, thereby increasing the diffusion distance of the ions, and reducing the oxygen diffusion rate in the material. Thus, the composites have good antioxidant properties. However, only relatively loose oxidized products are produced on the surface of composites at 800°C, and the contact of oxygen with the base material cannot be effectively isolated, which consequently worsens its antioxidant properties.

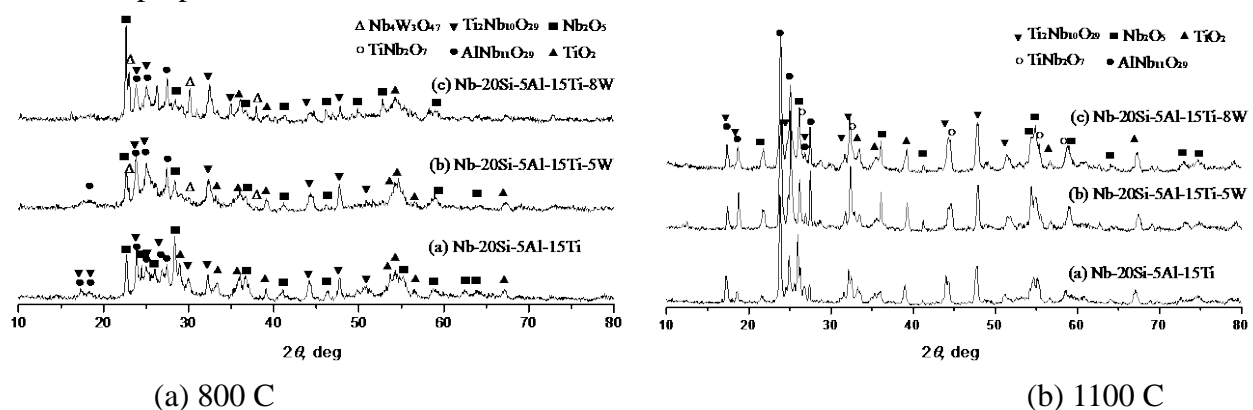


Fig.6. XRD patterns of the oxidized products.

The XRD patterns of the oxidized products at 800°C/100h and 1100°C/100h are shown in Fig.6. The oxidized products of the composites at 800°C are mainly composed of AlNb₁₁O₂₉, Ti₂Nb₁₀O₂₉, TiNb₂O₇, TiO₂, Nb₂O₅, and Nb₄W₃O₄₇; the oxidized products of the composites being oxidized at 1100°C are mainly composed of AlNb₁₁O₂₉, Ti₂Nb₁₀O₂₉, TiO₂, Nb₂O₅ and TiNb₂O₇. In addition, at 800°C, the peak intensity of Nb₂O₅ diffraction peak is much stronger than that at 1100°C. At 800°C, the oxidation product is dominated by Nb₂O₅. The molar volume of Nb is 10.9cm³, but that of Nb₂O₅ is 58.3cm³. The large volume expansion on oxidation of Nb naturally generates high stress at the alloy-oxide interface, and results in the cracking of Nb₂O₅ scale. The oxygen can easily diffuse in the Nb₂O₅ scale and Nb undergoes rapidly pest oxidation. So, the reduction of remaining Nb volume fraction can improve the oxidation resistance of Nb/Nb₅Si₃ in situ composites. At 1100°C, the Nb₂O₅ oxidized product is reduced, and the oxidized products of other alloy element are increased, therefore, a more dense oxide scale is formed and the oxidation resistance is enhanced.

Conclusions

(1) The Nb-20Si-5Al-15Ti-5Cr-xW composites that were prepared by using SPS is mainly composed of (Nb, Ti, W)_{ss}, α-Nb₅Si₃, and γ-Nb₅Si₃ phases and a small amount of (Nb, Ti)₅Si₃. At 800°C, the oxidized products are mainly composed of AlNb₁₁O₂₉, Ti₂Nb₁₀O₂₉, TiNb₂O₇, TiO₂, Nb₂O₅, and Nb₄W₃O₄₇. However, at 1100°C, the oxidized products are mainly composed of AlNb₁₁O₂₉, Ti₂Nb₁₀O₂₉, TiNb₂O₇, TiO₂, and Nb₂O₅.

(2) With an increase of W addition, the oxidation resistance of the composites at 800°C decrease

firstly and then increase. In the presence of 8 at.% W, the composite showed better oxidation resistance. At 1100°C the addition of W decreased the oxidation resistance during the first 40h, then changed to increase the oxidation resistance.

(3). In the presence of 8 at.% W, the Nb/Nb₅Si₃ composites to obtain dense and integrated oxide scales. In the formed oxide scales, the oxide of Nb was reduced, and the oxides of Al, Ti and W were increased. In addition, the compactness of oxide scales and adhesion were improved, which could effectively inhibit the diffusion of oxygen in the composite material, thereby improving the oxidation resistance of the material.

Acknowledgements

In this paper, the research was sponsored by the National Natural Science Foundation of China (Project No. 51271091) and the Nature Science Foundation of Jiangxi Province (Project No. GJJ12420) and the technology project of Jiangxi Province Education Department (Project No. 20161BAB206107).

References

- [1] Subramanian P R, Mendiratta M G, and Dimiduk D M. JOM[J], 1996, 48(1): 33~38.
- [2] Bewlay B P, Jackson M R, Subramanian PR. JOM[J], 1999; 51: 32.
- [3] Bewlay B P, Jackson M R, Zhao J-C, Subramanian P R. Metallurgical Mater Trans A[J], 2003, 34A: 2043-2052.
- [4] Rigney J D. Metall Trans A[J], 1996; 27A: 3292.
- [5] Liu Y. Mater Sci Eng A[J], 2010; A527: 1489.
- [6] Geng J, Tsakirooulos P, Shao G. Intermetallics[J], 2007, 15 (3): 69-76.
- [7] Zelenitsas K, Tsakirooulos P. Mater Sci Eng A[J], 2006, 416: 269-280.
- [8] Geng J, Tsakirooulos P, Shao G. Mater Sci Eng A[J], 2006, A441: 26-39.
- [9] J. Geng, P. Tsakirooulos, G. Shao. Mater. Sci. Eng. A[J], 2006, 441: 26~38.
- [10] Long W Y, Wan W D, Yao J P. Applied Mechanics and Materials[J], 2013, 376: 49-53.
- [11] Meier GH, Pettit FS. Mater Sci Eng A[J] 1992; 153(1-2): 548.
- [12] Grabke HJ, Meier GH. Oxid Met[J], 1995; 44(1-2): 147.
- [13] Meier GH. Mater Corros[J], 1996; 47(11): 595.
- [14] Geng J, Tsakirooulos P. Intermetallics[J], 2007; 15: 382.
- [15] Geng J, Tsakirooulos P, Shao G.. Intermetallics[J], 2007;15: 270.
- [16] Geng J, Tsakirooulos P, Shao G.. Intermetallics[J], 2007;15: 69.
- [17] Guo JT, Tian YX, Sheng LY, Zhou LZ, Ye HQ. Int J Mat Res[J], 2008;99:1275.
- [18] Knittel S, Mathieu S, Portebois L, Vilasi M. Intermetallics[J], 2014; 47: 43-52